Nucl. Phys. B 1025 (2026) 117386

Contents lists available at ScienceDirect

Nuclear Physics, Section B

journal homepage: www.elsevier.com/locate/nuclphysb

Quantum Field Theory and Statistical Systems

Nonextensive statistics and the finite-volume QCD phase transition

M.A.A. Ahmed [a,*], H. Zainuddin [b]

[a] Physics Department, Faculty of Science, Taiz University Al-Turba branch, Taiz, Yemen
[b] Department of Physics, Faculty of Science, Universiti Putra Malaysia (UPM), Selangor, Malaysia

ARTICLE INFO

Editor: Olalla Castro Alvaredo

Keywords:
Tsallis-Gibbs statistics
Finite volume
Partonic plasma and QCD

ABSTRACT

Recent studies have increasingly applied Tsallis nonextensive statistics to Quantum Chromodynamics (QCD) to account for deviations from thermal equilibrium. Within this framework, the Tsallis parameter $\mathfrak{q}$ characterizes long-range interactions, non-Markovian memory, and multifractal boundary effects; it links directly to temperature variances in fluctuating systems, which vanish in the Boltzmann-Gibbs limit. This study investigates the thermodynamic variables of a hot and dense system using the QCD MIT bag model, employing the Tsallis distribution to describe thermal response functions related to the equation of state. We focus on the deconfinement phase transition from a hadron gas to a Partonic Plasma to analyze the behavior of key thermodynamic quantities, such as energy and entropy densities, pressure, isothermal compressibility, and the interaction measure at finite volume. Furthermore, we examine the influence of the $\mathfrak{q}$-parameter on the phase transition point. Our findings reveal that the transition point is significantly shifted by the $\mathfrak{q}$-parameter, highlighting the importance of nonextensive statistics in characterizing the system's thermal evolution.

1. Introduction

Understanding the thermodynamical behavior of strongly interacting matter remains a central challenge in current nuclear and particle physics. Quantum chromodynamics (QCD) is the fundamental theory of strong interactions, accurately describing elementary particles, such as quarks and gluons, at the microscopic level. However, its inherently non-perturbative nature severely limits the possibility of direct analytical access to the overall thermodynamical properties of hadronic and particle matter [1–3]. Two emergent phenomena, color confinement and spontaneous breaking of chiral symmetries, dominate the low energy regime and govern the structure of hadrons and the QCD phase diagram [4]. Initial simulations of the lattice QCD provide an indispensable numerical view into QCD thermodynamics but are necessarily performed on finite and discrete spacetime volumes [5,6]. Lattice QCD (LQCD) simulations have achieved high precision at physical quark masses and show strong agreement with Relativistic Heavy Ion Collider (RHIC) and Large Hadron Collider (LHC) measurements, enabling reliable studies of dense QCD matter, including lattice Monte Carlo analyses of 2-color QCD at low temperatures [7–9]. Monte Carlo methods in statistical physics are based on probabilistic sampling and a small set of core algorithmic strategies, making them powerful tools for studying QCD at finite volume [10]. Thus, finite volume effects (FVE) are not simply technical products, but rather intrinsic features that must be carefully understood in order to extrapolate lattice results to the thermodynamical limit [11–13].

* Corresponding author.
E-mail addresses: mohammed_h7@taiz.edu.ye (M.A.A. Ahmed), Hishamuddinz@gmail.com (H. Zainuddin).

https://doi.org/10.1016/j.nuclphysb.2026.117386
Received 23 January 2026; Received in revised form 2 March 2026; Accepted 3 March 2026
Available online 15 March 2026

In addition to LQCD studies, finite spatial confinement arises naturally in many physical contexts, including RHIC, compact astronomical objects, and cosmology of the early universe, where the size of the system is often comparable to microscopic correlation lengths [14,15]. In high energy heavy ion collisions (HIC), statistical analyses of particle production provide evidence for the QCD phase boundary and support quark hadron duality at chemical freeze-out [16], while LQCD simulations precisely determine the equation of state (EoS) and conserved charge fluctuations near the transition temperature, firmly establishing the crossover nature of the QCD transition [17–21]. Recent LQCD studies have introduced a generalized definition of the isothermal compressibility in $(2+1)$-flavor QCD based on conserved charge fluctuations and show that, when normalized by pressure, isothermal compressibility remains close to the ideal gas limit in the vicinity of the pseudo critical temperature [22]. Earlier LQCD investigations of the EoS at finite chemical potential also report nontrivial behavior of the bulk isothermal compressibility across temperature and chemical potential [23]. These results underscore the importance of compressibility as thermodynamical response functions (TRFs) for strongly interacting matter near phase transitions and motivate detailed finite volume studies [22]. At the same time, Tsallis nonextensive statistics has been successfully applied to high-energy processes like proton-proton collisions and nuclear matter EoS, which naturally connects to thermofractal descriptions of QCD matter [24–27]. Notably, particle yields in central Au-Au collisions at RHIC were analyzed by comparing Boltzmann-Gibbs (BG) statistics with the Tsallis (TS) approach. By varying the nonextensive parameter within the range $1.01 \leq \mathfrak{q} \leq 1.25$, researchers found that the best agreement with experimental data occurred at $\mathfrak{q} = 1.16$. This result underscores the relevance of nonextensive effects as an underlying feature in the dynamics of HIC [28]. In these regimes, phenomenological models play an important complementary role. Among them, the MIT bag model offers a simple yet physically transparent description of quark confinement by introducing a vacuum pressure, the bag constant $\mathfrak{B}$, that balances the internal thermal pressure of the partonic [29,30]. Despite its simplicity, this model has been widely used to study the partonic EoS, deconfinement transitions, and partonic matter properties at finite temperatures [4,11,31]. However, most applications of the MIT bag model assume a thermodynamical limit, while systematic studies of finite size corrections remain relatively limited [19]. Nonextensive extensions of the MIT bag model based on TS successfully reproduce standard hadron masses and naturally extend to exotic multiquark states [18,21,32]. While incorporating a chemical potential dependent bag constant significantly alters neutron star matter, allowing isentropic hadronic and partonic phase transition. This modification ultimately yields stable partonic cores and the existence of massive compact stars compatible with current observations [33,34]. Conventionally, for thermodynamical calculations for a Bag Model system described by BG statistical mechanics with a partition function:

$$Z^{BG}(V;\beta,\mu) = \mathrm{Tr}[e^{-\beta(\hat{\mathcal{H}}-\mu_k\hat{N}_k)}], \tag{1}$$

where $\hat{\mathcal{H}}$ is the Hamiltonian of the system, β represents the average inverse temperature, k_B is Boltzmann's constant, μ_k is the chemical potential of the single-particle state k, and $\hat{N}_k$ is the number operator for each single-particle state k. At the same time, interest has grown in generalized statistical frameworks that go beyond BG thermodynamics. BG statistics rely on universality and the short term correlations, assumptions that may not apply to systems with strong, long-range, or nonequilibrium correlations [35]. Tsallis statistics provides a consistent generalization characterized by a nonextensivity parameter $\mathfrak{q}$ and has been successfully applied to a wide range of complex systems, including high energy hadronic collisions, nuclear matter, and astrophysical plasmas [36–39]. In the context of QCD, TS has been used to describe particle spectra, thermodynamically observable, and phase transition behavior, often resulting in improved apparent consistency [40,41]. Despite these developments, an important limitation remains. Most works incorporating TS in QCD-inspired models have implicitly taken into account infinite volume, thus ignoring the combined impact of confinement induced FVE and nonextensive statistical behavior. This omission is not insignificant: finite volume modifies the density of states and TRFs, while nonextensivity alters the statistical weighting of microstates. How these two effects interplay in determining the QCD phase structure remains largely unexplored.

In the BG limit ($\mathfrak{q} \to 1$), many conventional approaches ignore stability effects and finite size induced fluctuations, thereby overlooking the enhanced compressibility and mechanical softness expected for the partonic phase in small and dynamically evolving systems [42]. Although TS has been applied to the QCD equation of state [43] and to the QCD phase transition at finite temperature and chemical potential [44], important aspects of nonextensive effects on QCD thermodynamics remain insufficiently explored. Therefore, this work aims to address this problem by studying a finite volume formulation of the MIT bag model within the framework of TS. We systematically investigate the implications of this nonextensive approach for the phase transition between hadronic and partonic matter. Through systematic analysis of TRFs, such as pressure, energy density, entropy density, isothermal compressibility, and interaction measure, we investigate the interplay between FVE and nonextensive statistics in QCD-inspired systems. Our results demonstrate how deviations from BG extensivity modify the stability and phase structure of confined partonic matter and shift the deconfinement transition at finite volumes. This framework provides a unified and controlled description of the thermal QCD at finite size, enabling new insights into strongly interacting matter under extreme conditions and thus contributing to the formulation of a more appropriate EoS consistent with current RHIC phenomena.

2. Methodology

The BG is useful for studying many problems in physics. However, some phenomena require general statistics called nonextensive TS, which were introduced by Tsallis [35,45]. In TS, there are two additional features: the generalization of internal energy and BG entropy. However, there are $\mathfrak{q}$-deformed algebraic and/or quantum groups that allow the study of standard thermodynamics using a defined set of commutation and noncommutative relations and Jackson derivatives [46–48]. The theoretical framework of equilibrium statistical mechanics has found applications in many different areas of physics, such as elementary particle physics within QCD, string field theories, and chaos physics, including many-body physics [49–51]. It is well known that the partition function is a very important tool in statistical physics as Gibbs stated that the partition function contains all of the system's information [52]. New researchers have used the nonextensive TS as a validation test of the BG statistics, which is a specific instance of generalized statistical mechanics, when the Tsallis parameter $\mathfrak{q}$ is unity. The entropic parameter $\mathfrak{q}$ that describes the Tsallis distribution is connected to the relative temperature variance in a system of fluctuating temperature zones [36,53]. These fluctuations vanish for the BG distribution [36]. As mentioned before, TS is the generalization of BG statistics [35,45] whose entropy is

$$\mathcal{S}_{\mathfrak{q}} = k_B \frac{\mathrm{Tr}(\hat{\rho} - \hat{\rho}^{\mathfrak{q}})}{\mathfrak{q}-1}, \qquad (\mathfrak{q} \in \mathbb{R}), \tag{2}$$

where $\hat{\rho}$ is the Tsallis density matrix. The entropy $\mathcal{S}_{\mathfrak{q}}$ can be conveniently rewritten in the following alternative form:

$$\mathcal{S}_{\mathfrak{q}} = -k_B \,\mathrm{Tr}\Big(\hat{\rho}\, \ln_{\mathfrak{q}}^{(\gamma)} \hat{\rho}\Big), \tag{3}$$

where the $\mathfrak{q}$-logarithmic function is defined as follows:

$$\ln_{\mathfrak{q}}^{(\gamma)}(\hat{\rho}) = \begin{cases} \dfrac{\hat{\rho}^{\mathfrak{q}-1} - \mathbb{I}}{\mathfrak{q}-1}, & \text{for } \gamma = +, \\[2ex] \dfrac{\hat{\rho}^{1-\mathfrak{q}} - \mathbb{I}}{1-\mathfrak{q}}, & \text{for } \gamma = -, \end{cases}$$

with $\mathbb{I}$ denoting the identity operator. The parameter γ characterizes two regimes determined by the $\mathfrak{q}$-exponential and $\mathfrak{q}$-logarithmic functions [28,54]. In this work, we restrict our analysis to the positive regime of $\hat{\rho}$. In the limit $\mathfrak{q} \to 1$, the generalized logarithm reduces to the standard natural logarithm,

$$\lim_{\mathfrak{q}\to 1} \ln_{\mathfrak{q}}^{(\gamma)}(\hat{\rho}) = \ln(\hat{\rho}).$$

It is called a generalized logarithm because it is the inverse function of the generalized exponential,

$$e_{\mathfrak{q}}^{(\gamma)}(\hat{\rho}) = \begin{cases} \left[\mathbb{I} + (\mathfrak{q}-1)\hat{\rho}\right]^{\frac{1}{\mathfrak{q}-1}}, & \text{for } \gamma = +, \\[2ex] \left[\mathbb{I} + (1-\mathfrak{q})\hat{\rho}\right]^{\frac{1}{1-\mathfrak{q}}}, & \text{for } \gamma = -. \end{cases} \tag{4}$$

We consider a system $\mathfrak{s}$ composed of two independent subsystems, ($\mathfrak{s}_1$ and $\mathfrak{s}_2$). These subsystems are independent because they satisfy the density matrix relation $\hat{\rho}_{\mathfrak{q}}(\mathfrak{s}_1 \cup \mathfrak{s}_2) = \hat{\rho}_{\mathfrak{q}}(\mathfrak{s}_1) \otimes \hat{\rho}_{\mathfrak{q}}(\mathfrak{s}_2)$. For this configuration, the Tsallis entropy follows the specific non-additive relation provided below:

$$\mathcal{S}_{\mathfrak{q}}(\mathfrak{s}_1 \cup \mathfrak{s}_2) = \mathcal{S}_{\mathfrak{q}}(\mathfrak{s}_1) + \mathcal{S}_{\mathfrak{q}}(\mathfrak{s}_2) + (1-\mathfrak{q})\mathcal{S}_{\mathfrak{q}}(\mathfrak{s}_1)\mathcal{S}_{\mathfrak{q}}(\mathfrak{s}_2). \tag{5}$$

The aforementioned assumptions are tested in high-energy nuclear collisions, and experimental signals are observed that can be interpreted as a result of the presence of a nonextensive regime [55]. In $\mathfrak{q}$-equilibrium statistical mechanics, the essential object is the statistical density matrix $\hat{\rho}_{\mathfrak{q}}$

$$\hat{\rho}_{\mathfrak{q}}(V;\beta,\mu) = \frac{(\mathbb{I} + (\mathfrak{q}-1)\hat{\rho})^{\frac{1}{\mathfrak{q}-1}}}{Z_{\mathfrak{q}}(V;\beta,\mu)}. \tag{6}$$

We define the grand canonical partition function of the system in Eq. (1) via the density matrix in Eq. (6). Consequently, this leads to the Tsallis grand canonical partition function $Z_{\mathfrak{q}}(V;\beta,\mu)$. The Tsallis density matrix is employed to compute the ensemble average of any thermal observable. This observable is represented by the specific operator $\hat{A}$. Consequently, the average is defined as follows:

$$\langle\beta|\hat{A}|\beta\rangle_{\mathfrak{q}} = \frac{\mathrm{Tr}(\hat{A}\;\hat{\rho}_{\mathfrak{q}}(V;\beta,\mu))}{\mathrm{Tr}[\hat{\rho}_{\mathfrak{q}}(V;\beta,\mu)]}, \tag{7}$$

while the $\mathfrak{q}$-partition function of system is given by

$$Z_{\mathfrak{q}}(V;\beta,\mu) = \mathrm{Tr}'[\mathbb{I} + (\mathfrak{q}-1)\hat{\rho}]^{\frac{1}{\mathfrak{q}-1}}. \tag{8}$$

The stated trace in Eq. (8) imposes the Tsallis cut-off condition, which means that it is taken over the energy eigenvalues satisfying the constraint $1 + (\mathfrak{q}-1)\beta(\varepsilon-\mu) \geq 0$. When $\mathfrak{q} < 1$, the FD and BE distributions have a natural high-energy cut-off: $\varepsilon \leq 1/(\mathfrak{q}-1)\beta + \mu$, implying that the energy tail is depleted. When $\mathfrak{q} > 1$, the cut-off is absent, implying that the energy tail of the particle distribution is enhanced for fermions and bosons [55]. Now the grand canonical partition function for Bose-Einstein statistics is given by

$$Z_{\mathfrak{q}}^{(BE)}(V;\beta,\mu) \approx \left[\prod_{k=1}\right]_{\mathfrak{q}} \sum_{n_k=0}^{\infty} \left(e_{\mathfrak{q}}^{-\beta(\varepsilon_k-\mu)}\right)^{n_k}. \tag{9}$$

As we see in bosons case, each occupation number is assigned a value $n_k = 0, 1, 2, \cdots, N$ where occupation numbers satisfy

$$\sum_{k=1}^{\infty} n_k = N.$$

Also, the energy eigenvalues satisfy

$$\varepsilon = \sum_{k=1}^{\infty} n_k \varepsilon_k .$$

The sum in Eq. (9) is a geometric series, and has the value

$$\sum_{n_k=0}^{\infty} \left(e_{\mathfrak{q}}^{-\beta(\varepsilon_k-\mu)} \right)^{n_k} = \frac{1}{1 - e_{\mathfrak{q}}^{-\beta(\varepsilon_k-\mu)}}. \tag{10}$$

Hence, we can write Eq. (9) as

$$Z_{\mathfrak{q}}^{BE}(V;\beta,\mu) \approx \left[\prod_{k=1}\right]_{\mathfrak{q}} \frac{1}{1 - e_{\mathfrak{q}}^{-\beta(\varepsilon_k\mp\mu)}}. \tag{11}$$

On the other hand, for fermions the occupation numbers are restricted to the values $n_k = 0, 1$ because of Pauli's exclusion principle. For Fermi-Dirac statistics, one obtains,

$$Z_{\mathfrak{q}}^{FD}(V;\beta,\mu) = \left[\prod_{k=1}\right]_{\mathfrak{q}} \left(1 + e_{\mathfrak{q}}^{-\beta(\varepsilon_k\mp\mu)} \right), \tag{12}$$

Now, we can write both partition functions for the bosons and fermions in Eqs. (11) and (12) as

$$Z_{\mathfrak{q}}^{(\mathrm{BE,FD})}(V;\beta,\mu) \cong \left[\prod_{k=1}^{n}\right]_{\mathfrak{q}} \left(1 + \alpha e_{\mathfrak{q}}^{-\beta(\varepsilon_k\mp\mu)} \right)^{\alpha}. \tag{13}$$

The parameter α serves to interpolate between the two fundamental statistics. Specifically, the Bose-Einstein is recovered at $\alpha = -1$, whereas $\alpha = 1$ corresponds to the Fermi-Dirac. The mean number of the occupation number in TS is given by

$$\langle \hat{n}_{\mathfrak{q}}^{(\mathrm{BE,FD})} \rangle = n_{\mathfrak{q}}^{(\mathrm{BE,FD})}(V;\beta,\mu) \cong \frac{1}{(1-(\mathfrak{q}-1)\beta(\varepsilon\mp\mu))^{\delta} + \alpha}. \tag{14}$$

We must mention that the parameter $\delta = \dfrac{\mathfrak{q}}{\mathfrak{q}-1}$ can be obtained from the statistical mechanical formulations suggested by Tsallis in [27,56,57]. In contrast, another form of the parameter in $\delta = \dfrac{1}{\mathfrak{q}-1}$ will have a slightly different form of the Tsallis quantum distributions [40,58–64].

Now we introduce the partition function of our system. In this study, we have taken the hadronic gas, which is considered an ideal relativistic gas of massless pions, whereas the PP phase is merely a free partonic system. We employ a basic Phase Coexistence Model (PCM) from [15], in which the mixed-phase system has a finite size $V = V_{HG} + V_{PP}$. The fraction of volume occupied by the HG phase (specified by the parameter h) is $V_{HG} = hV$, while the remaining volume is $V_{PP} = (1-h)V$, which contains the PP phase. The total partition function of the system can be expressed as a product of two partition functions if the reciprocal interactions between the various phases are ignored, as follows:

$$Z_{\mathfrak{q}}^{\mathrm{SYS}}(h,T,V,\mu) = Z_{\mathfrak{q}}^{PP}(h,V;T,\mu) Z_{\mathfrak{q}}^{HG}(h,V;T,\mu). \tag{15}$$

The difference between the real vacuum and the perturbative vacuum due to color confinement implies that the constant ($\mathfrak{B}$) of the bag model represents the pressure on the surface of the bag to balance the outward pressure exerted by partons moving inside the bag. A non-variable Bag constant $\mathfrak{B}^{1/4}$ is insufficient because the non-abelian nature of QCD leads to a complicated and non-perturbative structure of the QCD vacuum. In this work, we have always taken into account a constant value equal to 145 MeV, as this value is known to lie within the stability window that satisfies the Bodmer-Witten conjecture [65]. For a PP consisting of gluons and two flavors of massless quarks (up, down) without a chemical potential μ in the bag model. The total Tsallis partition function (see Appendix A), $Z_{\mathfrak{q}}^{\mathrm{SYS}}(h,V;T)$, of the whole system can be written as:

$$Z_{\mathfrak{q}}^{\mathrm{SYS}}(h,V;T) = \exp\left(VT^3 \left[\left\{ -\frac{1}{\pi^2}\left(\frac{13}{6}T_{\mathfrak{q}}^{B} + 2T_{\mathfrak{q}}^{F}\right) + \frac{\mathfrak{B}}{T^4} \right\} h + \left\{ \frac{2}{\pi^2}\left(\frac{4}{3}T_{\mathfrak{q}}^{B} + 2T_{\mathfrak{q}}^{F}\right) - \frac{\mathfrak{B}}{T^4} \right\} \right] \right). \tag{16}$$

The $\mathfrak{q}$-generalized special functions T_q^B and T_q^F correspond to boson and fermion cases, respectively. Now, we define the Tsallis Hadronic Probability Density Function (THPDF) is given by

$$\varrho_{\mathfrak{q}}(h,V;T) = \frac{Z_{\mathfrak{q}}^{\mathrm{SYS}}(h,V;T)}{\int_0^1 Z_{\mathfrak{q}}^{\mathrm{SYS}}(h,V;T)\,dh}. \tag{17}$$

Because our THPDF is directly connected to the Tsallis partition function of the system, it is assumed that it contains all of the information about QCD matter and its deconfinement phase transition. The mean value of any TRFs may therefore be calculated as follows:

$$Q_{\mathfrak{q}}(V;T) = \int_0^1 Q(h,V;T)\varrho_{\mathfrak{q}}(h,V;T)\,dh, \tag{18}$$

where $Q_q(V;T)$ describes the system in the state h. By employing Eq. (18), the mean value is redefined, and the expectation value of the observable A for the complete system can be written as

$$Q_q^A(V;T) = \int_0^1 Q^A(h,V;T) P_q(h,V;T) dh. \tag{19}$$

The expectation value of the observable A for the sub-system (A-only) is given by

$$\mathfrak{Q}_q^A(V;T) = \int_0^1 \mathfrak{Q}^A(h,V;T) p_q^A(h,V;T) dh. \tag{20}$$

If we are studying subsystem A (pions, vacuum, quarks, or gluons) when the entire system is functioning, we use Eq. (19). However, when we are studying only system A, the single active component, we use Eq. (20). Using the THPDF of the system as shown in Eq. (17) and the expressions in Eqs. (19) and (20), the TRFs have two different ways. In statistical mechanics and critical phenomena, infinite systems exhibit true singularities of the TRFs (e.g., the divergence of heat capacity or susceptibility). However, in finite-size systems, these singularities are rounded and shifted, producing finite peaks instead of true divergences. This behavior is captured in the finite-size scaling theory, which relates the system size $L = V^{1/d}$ to deviations from critical behavior in the thermodynamical limit. These singularities are converted into finite peaks with well-defined amplitudes and widths, in addition to the scaling of the thermodynamical quantities, when they are investigated as TRFs at finite size [66–70]. The system under study and produced in Ultra-RHIC) expands as soon as it is created. It includes many particles of small finite sizes on both sides of the deconfinement phase transition (partons in the PP and pions in the HG). If these particles interact strongly enough, the system may achieve local thermodynamical equilibrium. Relativistic hydrodynamics can readily represent the subsequent evolution of the PP and HG if they are locally maintained during later growth. Hydrodynamics is a macroscopic method that characterizes a system using macroscopic quantities such as local energy density $\varepsilon_q(V;T)$, pressure $p_q(V;T)$, dynamical number of degrees of freedom, and entropy density $s_q(V;T)$. This requires an EoS, which establishes a relationship between pressure, energy, and entropy but does not provide in-depth details of the microscopic dynamics. In general, we require an EoS to represent the hydrodynamic expansion of a system of particles in collisions from phenomenological methods to URHIC physics. The type of EoS has a major influence on the space-time pattern of a collision, and the phase transition increases the collision duration. A detailed study of the temperature dependence of some TRFs, such as pressure $p_q(V;T)$ and energy density $\varepsilon_q(V;T)$ is needed for details of these thermal functions in experimental and theoretical studies. Thus, we will choose some TRFs to evaluate their phase transition at finite size using TS.

2.1. The some thermal response functions of the system

The mean value of the hadronic volume fraction $H_q(V;T)$, which is used as the order parameter for the phase transition studied in this work, is the first quantity considered in our research. These quantities can be wirtten according to Eqs. (17) and (18) by,

$$H_q(V;T) = \langle h(V;T) \rangle = \int_0^1 h\, \varrho_q(h,V;T) dh. \tag{21}$$

On integration, Eq. (21) reads,

$$H_q(V;T) = \frac{1}{VT^3\left(\frac{1}{\pi^2}\left[\frac{13}{6}T_q^B + 2T_q^F\right] - \frac{\mathfrak{B}}{T^4}\right)} + \frac{1}{1 - \exp^{VT^3\left(\frac{1}{\pi^2}\left[\frac{13}{6}T_q^B + 2T_q^F\right] - \frac{\mathfrak{B}}{T^4}\right)}}. \tag{22}$$

We will see that the most important physical quantities can be obtained via this fundamental quantity, which is considered an order parameter. Now, we introduce the energy density $\varepsilon_q(V;T)$, whose mean value was also computed in the same manner and was confirmed to be related to $H_q(V;T)$ through the relation

$$\varepsilon_q(V;T) = \frac{T^2}{V}\left\langle \frac{\partial}{\partial T}\left(\ln Z_q^{\mathrm{SYS}}(h,V;T)\right)\right\rangle. \tag{23}$$

After using Eq. (23) the density energy will be given by

$$\frac{\varepsilon_q(V;T)}{T^4} = \left(\left(\frac{6}{\pi^2}\left[\frac{4}{3}T_q^B + 2T_q^F\right] + \frac{\mathfrak{B}}{T^4}\right) - \left(\frac{3}{\pi^2}\left[\frac{13}{6}T_q^B + 2T_q^F\right] + \frac{\mathfrak{B}}{T^4}\right) H_q(V;T)\right). \tag{24}$$

We note the Eq. (24) has an important form of the normalized energy density of the system $\varepsilon_q(V;T)/T^4$. We now turn to another TRF, namely the entropy density $s_q(V;T)$, which can be evaluated within the same theoretical framework using its standard thermodynamical definition.

$$s_q(V;T) = \frac{1}{V}\left\langle \frac{\partial}{\partial T}\left(T \ln Z_q^{\mathrm{SYS}}(h,V;T)\right)\right\rangle. \tag{25}$$

The entropy density is related to the order parameter, so after using Eq. (25), the entropy density can be written as

$$\frac{s_q(V;T)}{T^3} = \frac{8}{\pi^2}\left(\left[\frac{4}{3}T_q^B + 2T_q^F\right] - \left[\frac{13}{12}T_q^B + T_q^F\right] H_q(V;T)\right). \tag{26}$$

The definition of the pressure in thermodynamical is given by [71,72]

$$p_{\mathfrak{q}}(V;T) = T\left\langle \frac{\partial}{\partial V}\left(\ln Z_{\mathfrak{q}}^{\mathrm{SYS}}(h,V;T)\right)\right\rangle, \tag{27}$$

and after a simple calculation, we obtain the final formal of the total pressure,

$$\frac{p_{\mathfrak{q}}(V;T)}{T^4} = \left(\left(\frac{2}{\pi^2}\left[\frac{4}{3}T_{\mathfrak{q}}^{B} + 2T_{\mathfrak{q}}^{F}\right] - \frac{\mathfrak{B}}{T^4}\right) - \left(\frac{1}{\pi^2}\left[\frac{13}{6}T_{\mathfrak{q}}^{B} + 2T_{\mathfrak{q}}^{F}\right] - \frac{\mathfrak{B}}{T^4}\right)H_{\mathfrak{q}}(V;T)\right), \tag{28}$$

which shows the contribution of the pressure $p_{\mathfrak{q}}(V;T)$ during phase transition in our system. For a homogeneous and isotropic QCD matter in thermal equilibrium, the expectation value of the energy-momentum tensor can be written in partonic matter form as

$$\theta^{\mu\nu} = (\varepsilon + p)\,u^{\mu}u^{\nu} - p\,g^{\mu\nu}, \tag{29}$$

where u^{μ} is the four velocity of the matter. The FVE enter through the volume dependence of the thermodynamical quantities ε and p, while the tensor structure remains unchanged. The trace of the energy momentum tensor is obtained by contracting with the metric tensor,

$$\theta^{\mu}{}_{\mu} = g_{\mu\nu}\theta^{\mu\nu}. \tag{30}$$

By substituting into Eq. (29), and then using $u^{\mu}u_{\mu} = 1$ and $g^{\mu}{}_{\mu} = 4$ in four dimensions of spacetime, we find

$$\theta^{\mu}{}_{\mu} = (\varepsilon + p) - 4p = \varepsilon - 3p. \tag{31}$$

We now conclude the difference between Eq. (24) and 3 Eq. (28) is an interaction measure, which is also known as the trace anomaly $\theta_{\mathfrak{q}}(V;T)$,

$$\theta_{\mathfrak{q}}(T;V) = 4\mathfrak{B}\big(1 - H_{\mathfrak{q}}(V;T)\big). \tag{32}$$

This quantity is vanishing in massless gas and non-interacting, whereas it appears in the case of an interacting system. The relationship between the non-zero value of the interaction measure and TS and the vacuum contribution has been thoroughly understood in the QCD MIT Bag Model. The expression $4\mathfrak{B}(1 - H_{\mathfrak{q}}(V;T)$ appears in our EoS, where $(1 - H_{\mathfrak{q}}(V;T))$ represents the term of PP. This term distinguishes itself from the variation with the EoS, commonly used: $3p_{\mathfrak{q}}(V;T) = \varepsilon_{\mathfrak{q}}(V;T)$. It is related to everything that occurs during the deconfinement phase transition, therefore its non-perturbative origin is obvious.

2.2. The pressure and the compressibility of the subsystem

Now, we show the very important TRF which called the isothermal compressibility. This quantity is defined as

$$K_{\mathfrak{q}}^{-1}(V;T) = \upsilon\left(V\frac{\partial}{\partial V}\left(P_{\mathfrak{q}}(V;T)\right)\right). \tag{33}$$

In the analysis of the PP, the parameter υ enforces the fundamental mechanical stability condition. It ensures that the isothermal bulk modulus, defined via Eq. (33), remains a positive-definite quantity during high energy density fluctuations. For both the PP and HG phases, thermodynamic consistency requires a negative volumetric pressure response, where $(\partial P_{\mathfrak{q}}/\partial V)_T < 0$. By adopting the convention $(\upsilon = -1)$, the formalism aligns non-extensive pressure derivatives with standard global stability criteria. This choice correctly captures the restoring force of the $\mathfrak{q}$-generalized medium against volumetric perturbations. Furthermore, it ensures the sign conventions are fully compatible with the underlying statistical mechanics of the non-extensive ensemble. Accordingly, the isothermal compressibility for QCD matter across the HG and PP transition is naturally extended by defining it at fixed temperature and a fixed conserved flavor quantum numbers within the TS ensemble. This helps us determine the compressibility of PP in the bag model. If we are studying subsystem A (pions, vacuum, quarks, or gluons) when the entire system is functioning, we use Eq. (19). However, when we are studying only system A, the single active component, we use Eq. (20). Using the THPDF of the system as shown in Eq. (17) and the expressions in Eqs. (19) and (20), the pressure shown in Eq. (27) can be interpreted in two ways at a typical temperature.

$$P_{\mathfrak{q}}^{A}(V;T) = T\int_0^1 \left(\frac{\partial}{\partial V}\left(\ln Z_{\mathfrak{q}}^{A}(h,V;T)\right)\right)\varrho_{\mathfrak{q}}(h,V;T)dh, \tag{34}$$

and

$$p_{\mathfrak{q}}^{A}(V;T) = T\int_0^1 \left(\frac{\partial}{\partial V}\left(\ln Z_{\mathfrak{q}}^{A}(h,V;T)\right)\right)\varrho_{\mathfrak{q}}^{A}(h,V;T)dh. \tag{35}$$

Hence, equating subsystem pressure in full system and/or subsystem pressure with itself, given by Eqs. (34) and (35) respectively.

3. Results

3.1. The energy and entropy densities, pressure, and the trace anomaly of the system

At low temperatures $T \approx (0.08 - 0.10)$GeV, the order parameter saturates near unity, indicating that the system remains entirely in the HG phase. As the temperature increases toward the critical region $T \approx 0.12$GeV, the order parameter decreases sharply, signaling the onset of the deconfinement transition, where hadrons disintegrate into quarks and gluons to form the PP. Beyond the critical

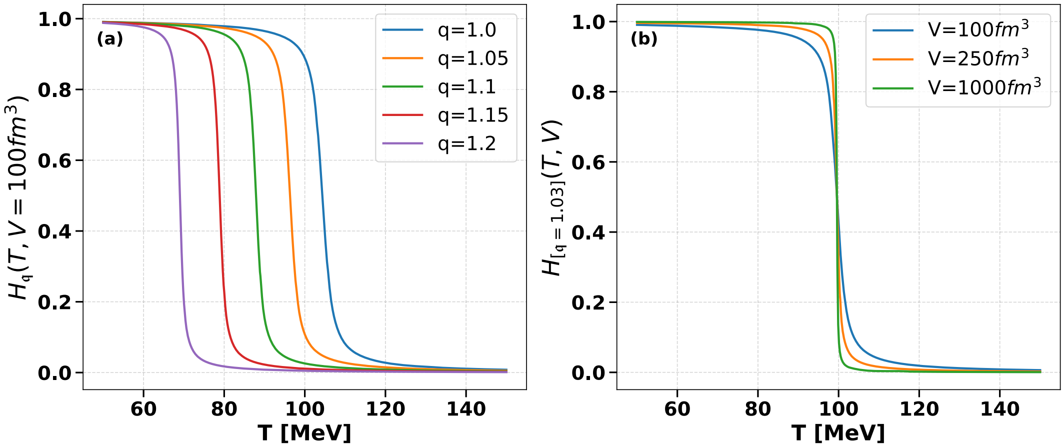

Fig. 1. (a) The order parameter versus temperature T, when $V = (0.1fm)^3$ with set Tsallis parameter $\mathfrak{q} = (1.00, 1.05, 1.10, 1.15, 1.20)$. (b) The order parameter as a function of temperature T at $\mathfrak{q} = 1.03$ for volumes $V = (0.1, 0.25, 1)(10fm)^3$.

Table 1
$T_0(V)$ is the temperature of the transition point for different Tsallis parameter values with volume.

q-parameter	$T_0(V = (0.1\text{fm})^3)$ [MeV]
$\mathfrak{q} = 0.99$	105.9073 ± 0.00001
$\mathfrak{q} = 1.00$	104.3480 ± 0.00001
$\mathfrak{q} = 1.03$	99.5862 ± 0.00001
$\mathfrak{q} = 1.07$	93.0175 ± 0.00001
$\mathfrak{q} = 1.11$	86.1451 ± 0.00001
$\mathfrak{q} = 1.15$	78.8818 ± 0.00001
$\mathfrak{q} = 1.19$	71.0810 ± 0.00001

temperature T_0, the order parameter becomes small, indicating that the system predominantly resides in the PP phase at higher temperatures. Thus, the order parameter serves as a quantitative measure of the degree of deconfinement approaching unity in the HG phase, vanishing in the PP phase, and taking intermediate values in the mixed transition region. Fig. 1(a) illustrates the behavior of the order parameter $H_\mathfrak{q}(V;T)$ at a fixed volume. We observe that the transition point is highly sensitive to the non-extensivity parameter $\mathfrak{q}$. In contrast, the order parameter is plotted as a function of temperature T at a fixed $\mathfrak{q} = 1.03$ for various volumes in Fig. 1(b). As the volume V increases from 100 fm^3 to 1000 fm^3, the transition from the HG to the PP becomes noticeably sharper. This trend indicates that larger system volumes reduce FVE, causing the transition width to narrow as the system approaches the thermodynamical limit. Meanwhile, the figure demonstrates that variations in system volume do not shift the transition point for a constant value of $\mathfrak{q}$. These results indicate that while the thermal equilibrium of the system is $\mathfrak{q}$-dependent, the critical transition temperature remains invariant with respect to the system volume. We can consider that the transition point as being the point in which we have equal probability of hadronic phase and PP phase: $H_\mathfrak{q}(V;T) = 1 - H_\mathfrak{q}(V;T)$. Thus, $H_\mathfrak{q}(T_0(V)) = 1/2$ determines the value of the order parameter for both phases. Moreover, we know that the order parameter has a finite discontinuity in the thermodynamical limit, which can be expressed in terms of a step function: $\lim_{V\to\infty}\left[H_{\mathfrak{q}\to 1}(V;T) = 1 - \Theta(T - T_0(\infty))\right]$.

In the table (1), the transition temperature for different $\mathfrak{q}$ values in a volume of 100 fm^3. Although we take into account the color state of PP, the transition point shift occurs for different values of $\mathfrak{q}$ at the same volume, but in related works, the transition point shift occurred when we took into account the colorless state of PP for different volumes within BG statistics [68–70]. In this work, we focus on $\mathfrak{q} \geq 1$ and emphasize that the physically relevant range for HIC is $(1 \leq \mathfrak{q} \leq 1.2)$ [28,73,74].

Traditionally, the quantity $\varepsilon_\mathfrak{q}(V;T)/T^4$ is interpreted as the number of effective degrees of freedom in the system. The liberation/melting of the partonic degrees of freedom locked in the hadronic phase during the QCD deconfinement phase transition is visually suggested in Fig. 2. In the thermodynamical limit, this deconfinement causes a finite smooth jump in finite volume to become a sharp discontinuity, which is connected to the latent heat of the first-order deconfinement phase transition. Over virtually the entire temperature range, there was a strong size dependency. With the increase of the $\mathfrak{q}$-values, the energy density $\varepsilon_\mathfrak{q}/T^4$ grows faster, exhibiting a continuous abrupt increase in its value for particular temperatures, suggesting a probable shift to greater degrees of freedom. For all $\mathfrak{q}$-values, after reaching a maximum value of energy density, it starts to drop at higher temperatures and moves to a saturation zone. This conduct can be understood as follows. As the temperature increases, more and more heavy resonances start contributing to the $\varepsilon_\mathfrak{q}/T^4$, and therefore one sees a strong increase in the $\varepsilon_\mathfrak{q}/T^4$. At sufficiently high temperature, the system starts to act like a gas of massless particles, and $\varepsilon_\mathfrak{q}/T^4$ finally goes to a constant value. The fast increase with the parameter $\mathfrak{q}$ happens

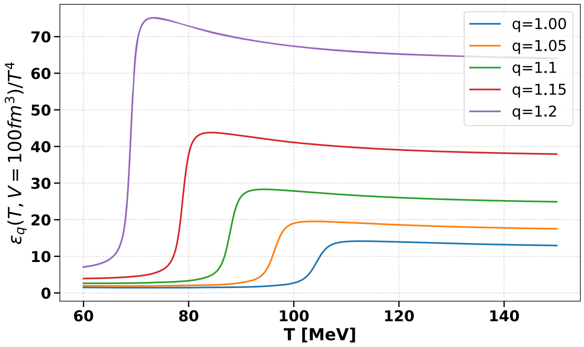

Fig. 2. Normalized energy density $\frac{\epsilon_q(V;T)}{T^4}$ versus temperature T, when $V = (0.1 fm)^3$ with set Tsallis parameter $\mathfrak{q} = (1.00, 1.05, 1.10, 1.15, 1.2)$.

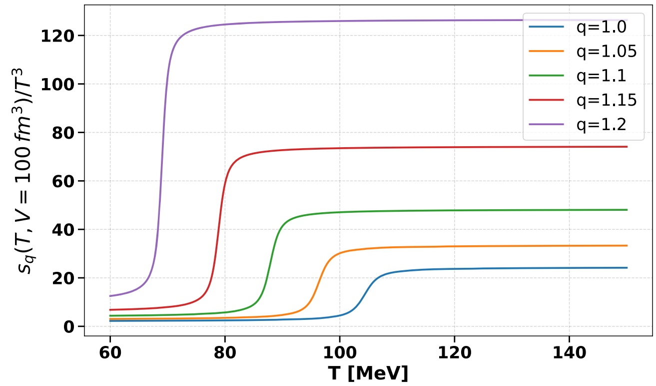

Fig. 3. Normalized entropy density $\frac{s_q(V;T)}{T^3}$ versus temperature T, when $V = (0.1 fm)^3$ with set Tsallis parameter $\mathfrak{q} = (1.00, 1.05, 1.10, 1.15, 1.20)$.

because the distribution deviates more and more from a Boltzmann distribution and the tails with large momentum contribute more and more as $\mathfrak{q}$ grows.

Traditionally, the quantity $s_q(V;T)/T^3$ has been interpreted as a measure of the number of effective degrees of freedom in the system. The liberation/melting of the partonic degrees of freedom locked in the hadronic phase, as seen in Fig. 3 of the normalised entropy density in the QCD deconfinement phase transition, is logically persuasive. In the thermodynamical limit, this deconfinement causes a finite smooth jump at finite size to become a finite sharp discontinuity, which is connected to the latent heat of the first-order deconfinement phase transition. Over virtually the entire temperature range, there is a strong size dependency. When approaching the thermodynamical limit, the first-order character of the transition temperature is given by the step-like rise or sharp discontinuity of each of the order parameter, as well as the normalised energy and entropy densities. This reflects the presence of latent heat accompanying the phase transition. The quantities ϵ_q/T^4 and s_q/T^3 are traditionally interpreted as a measure of the number of effective degrees of freedom [75]. The temperature rise causes "melting" of the constituent degrees of freedom "frozen" in the hadronic case, causing the energy and entropy densities to reach their plasma values. Because of the significant thermodynamical fluctuations, the probability of the presence of the PP phase below the critical point, and of the pionic phase above the critical point are limited in small systems, the phase transition is smoothened. The plot of the estimated pressure normalised by T^4 is shown in Fig. 4. Just after the transition temperature, and especially when the volume approaches the thermodynamical limit, a fast increase in pressure can be noticed.

It is obvious that below the transition temperature, the pressure remains constant with the Stefan Boltzmann (SB) value in the HG phase, then it rapidly increases at $T_0(V)$ and continues to grow, albeit slowly. As a function of temperature, the pressure continued to increase monotonically, a behaviour that is compatible with the phenomenon of phase coexistence. The behavior of p_q/T^4 is shown in Fig. 4 for different values of $\mathfrak{q}$ where its response increases with temperature growth and different values of $\mathfrak{q}$ and gradually stabilizes. The Figs. 2, 3, and 4 all exhibit a characteristic S-shaped growth as temperature T increases. This smooth transition, rather than a sharp jump, is a direct result of the rounding and widening effects caused by the finite volume. As the non-extensivity parameter $\mathfrak{q}$ increases from 1.00 to 1.2, all three quantities demonstrate a significant shifting effect, where the transition to the high-temperature phase begins at progressively lower temperatures. Additionally, higher values of $\mathfrak{q}$ lead to higher saturation magnitudes for these normalized densities, suggesting that $\mathfrak{q}$ scales the effective degrees of freedom within the system. Moreover, we note from those figures, when $\mathfrak{q}$ goes to unit, p_q/T^4, ϵ_q/T^4, and s_q/T^3, all tend to their SB limit. However, as $\mathfrak{q}$ increases, the quantities increased rapidly until they exceed their corresponding SB limits. Taking ϵ_q/T^4 as an example, for the QCD deconfinement phase transition

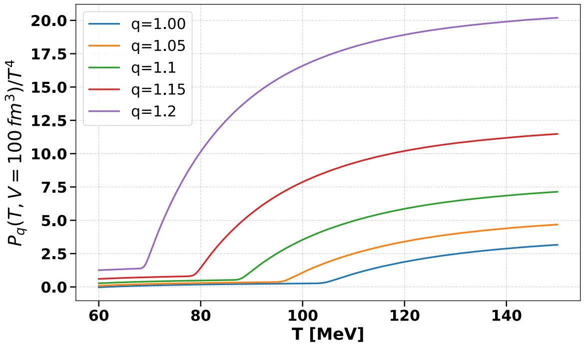

Fig. 4. Normalized pressure $\frac{p_q(V;T)}{T^4}$ versus temperature T, when $V = (0.1 fm)^3$ with set Tsallis parameter $q = (1.00, 1.05, 1.10, 1.15, 1.20)$.

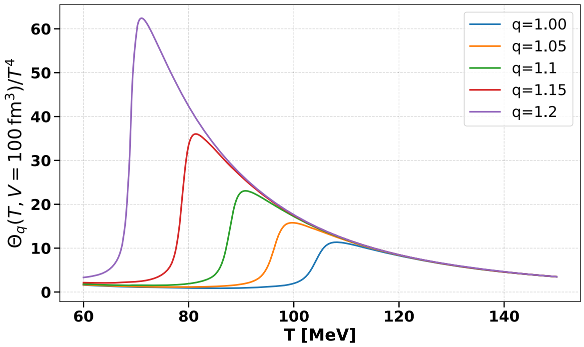

Fig. 5. Trace anomaly $\frac{\theta_q(V;T)}{T^4}$ versus temperature T, when $V = (0.1 fm)^3$ with set Tsallis parameter $q = (1.00, 1.05, 1.10, 1.15, 1.20)$.

from HG to PP and the temperature is fixed at 0.15 GeV. When $q = 1$, the value of ε_q/T^4 is 13.036, very close to the SB limit 12.18. But when $q = 1.1$, the value of ε_q/T^4 is 24.973 i.e. increased by 91%.

Furthermore, from Figs. 2 and 3, we find that the response patterns of the energy and entropy densities for q are almost the same. They reach a maximum near the transition point T_0, then decrease and tend to be stable.

The graph in Fig. 5 shows the interaction measure $\theta_q(V;T)/T^4$ as a function of temperature for various values of the Tsallis parameter. Our findings appear to be in good convention with the interaction measure known behaviour. In particular, $\theta_q(V;T)/T^4$ increases rapidly beyond the transition point with the values of Tsallis parameter. Subsequently, it decreases slowly at high temperatures, leading to the emergence of a maximum slightly above the transition region. The position of this maximum depends on the value of the Tsallis parameter. This behavior is a direct result of the FVE, which changes how phase transitions occur when the system is at finite volume. In particular, θ_q/T^4 shows a clear peak. This peak illustrates how finite size smooths out singular behavior: in an infinite system, a second-order transition could diverge, but in a finite system, the divergence is replaced by a finite peak because the volume is finite. As q increases, the peak shifts to a lower temperature T, and it also becomes higher and narrower. This means that finite volume still smooths the singularity, but a larger q strengthens the critical behavior and makes the transition look sharper even in a finite volume. At both low and high temperatures, the Tsallis parameter dependency is small, as seen in Fig. 5. However, in the middle area, about the maximum, this dependency is more prominent. The system is not in an optimal condition just above the Tsallis parameter transition temperature. The mutual interactions between partons result in a non-vanishing interaction measure, which agrees well with many models, such as hot lattice QCD computations. The fact that the pressure, energy, and entropy densities of the PP remain significantly below their corresponding ideal gas values, even at high temperatures, indicates the persistence of strong residual QCD interactions among the partons. In other words, the partons continue to "feel" each other despite the high-temperature environment. The q-parameter acts as a proxy for the long-range correlations and collective effects that are intrinsic to QCD dynamics. This interpretation is quantitatively supported by the non-vanishing interaction measure Θ_q/T^4 and the observed deviation from the ideal gas limit, which together characterize the PP as a strongly correlated, non-ideal system. The interaction measure is related to p_q/ε_q, this quantity help to measures the deviation from EoS of an ideal gas $\varepsilon_q = 3p_q$ due to interactions and/or finite quark masses.

3.2. The pressure and compressibility of the subsystem

The pressure and the bag constant play a central role in describing deconfinement. Within the MIT Bag Model, the confined phase is stabilized by the negative vacuum pressure encoded in the bag constant, whereas the PP phase is dominated by the thermal pressure of quarks and gluons treated as a relativistic gas [29]. The phase transition occurs when the partonic pressure becomes equal to the vacuum pressure, signaling the dissolution of hadronic bags. When implemented in TS, the effective pressure of the partonic medium

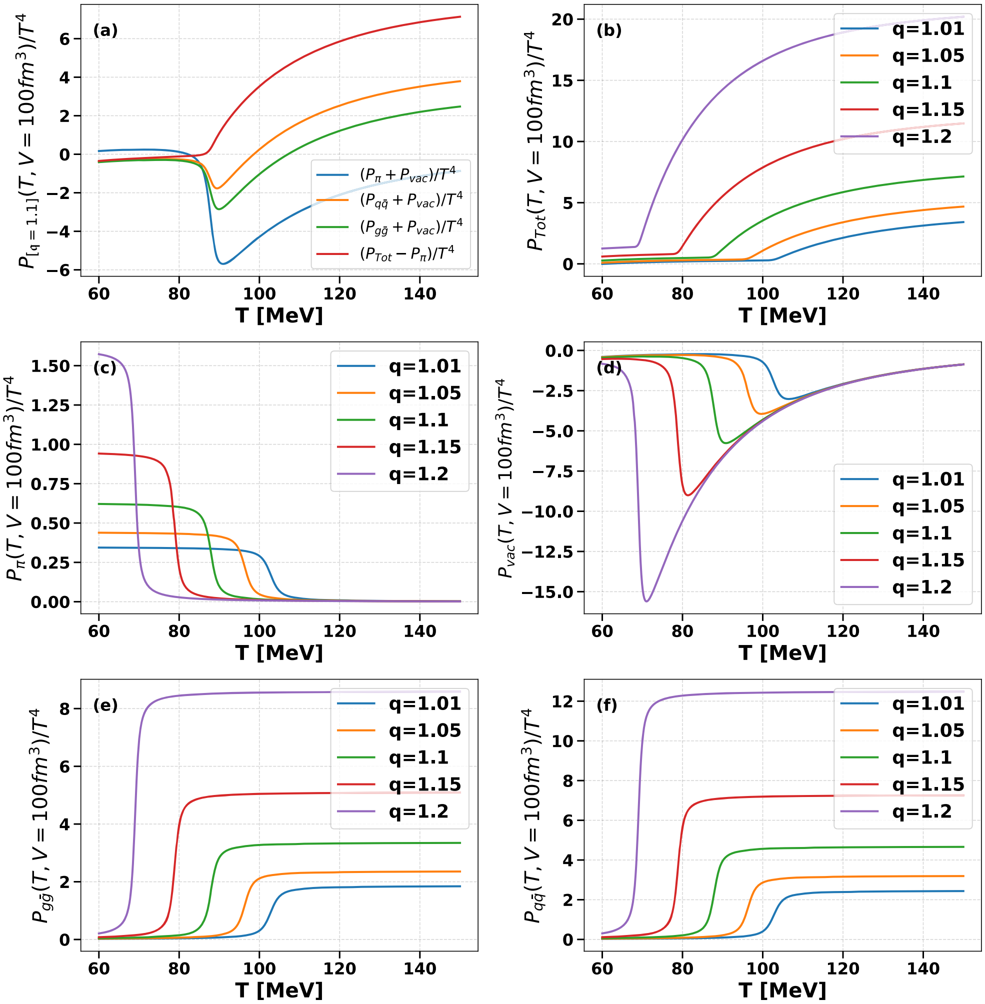

Fig. 6. (a) The plot of the vacuum pressure with (pion or quarks, and/or gluons) pressures of the system as a function of $(T, q = 1.1; V = (0.1\text{fm})^3)$. Panels (b)-(f) show the plots of the total pressure, pion pressure, vacuum pressure, gluon pressure, and quark pressure of the system, respectively, as functions of (q, T) at a fixed volume $V = (0.1\text{fm})^3$.

is modified by the q-parameter, which shifts the condition (gas pressure equals vacuum pressure) and alters both the EoS and the deconfinement threshold between the HG and PP [35,76].

The total pressure of the system is constructed as the sum of the partial pressures of the pions, quarks, gluons, and the QCD vacuum. Fig. 6 shows each being evaluated using the appropriate THPDF [35,76]. In the confined phase, the pressure is dominated by the pionic contribution arising from Tsallis-modified Bose statistics, while quark and gluon pressures remain suppressed. The vacuum pressure enters through the bag constant $\mathfrak{B}$, which acts as a negative pressure for $\mathfrak{B} > 0$, contributing to the stability of the hadronic matter by balancing the external thermal pressure of the pion gas [14,29]. As the temperature increases toward deconfinement, the Tsallis-modified pressures of quarks and gluons grow rapidly and eventually dominate the EoS, whereas the vacuum contribution remains fixed [77]. Conversely, the negative bag constant $\mathfrak{B} < 0$ corresponds to an effective positive vacuum pressure, enhancing the total pressure and favoring the onset of deconfinement [78]. Fig. 7 illustrates the pressure behavior when the THPDF of the entire system is employed. The pressure of each component of the pion, partonic, and vacuum is evaluated as a weighted expectation value over all possible phase configurations, taking into account phase coexistence and statistical mixing near the transition region [76]. When using the THPDF for a single subsystem (pions, quarks, gluons, or vacuum), the resulting pressure represents the intrinsic contribution of that isolated component alone. Thermodynamical consistency, at equilibrium, requires that the pressure of each subsystem integrated into the whole system equal its pressure when treated independently, thus ensuring mechanical equilibrium between the degrees of freedom of pion, partonic, and vacuum across the pionic gas PP phase transition.

When a strongly interacting matter undergoes a phase transition from the HG phase to the PP phase, significant modifications occur in its thermodynamical properties, most notably its pressure and isothermal compressibility [78]. Consequently, at finite energy density, the pressure in the PP phase is generally expected to exceed the pressure in the HG phase, reflecting the substantially larger

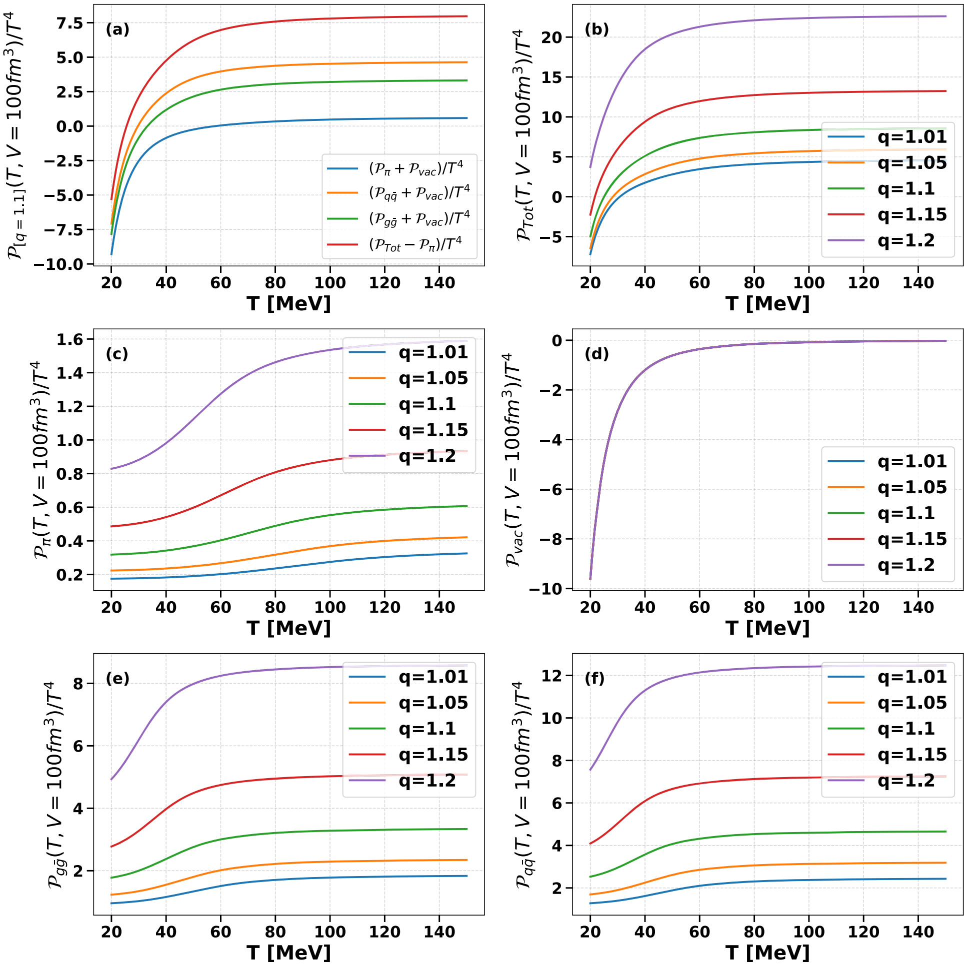

Fig. 7. (a) Vacuum pressure, together with (pion, quark-antiquark and/or gluon-antigluon) pressures for the sub-system, at fixed ($q = 1.1; V = (0.1\text{fm})^3$). (b)-(f) The plots for ($p_{tot}(T)/T^4, p_\pi(T)/T^4, p_{vac}(T)/T^4, p_{g\bar{g}}(T)/T^4$, and $p_{q\bar{q}}(T)/T^4$) of the sub-system, respectively, at a fixed volume $V = (0.1\text{fm})^3$ for $q \in \{1.01, 1.05, 1.10, 1.15$ and $1.20\}$.

number of microscopic degrees of freedom available in deconfined QCD matter [79]. The isothermal compressibility determines the volume response of a system to pressure changes at finite temperature and thus provides a sensitive tool for studying phase transitions, which are often accompanied by singular behavior or pronounced changes in thermodynamical observables [80]. In the case of a first-order phase transition, isothermal compressibility may diverge, reflecting phase coexistence and the emergence of large fluctuations in volume or density occurring without a corresponding change in pressure [81]. By contrast, for a smooth crossover transition widely accepted to describe the QCD phase transition at vanishing or small baryon chemical potential, isothermal compressibility remains finite but exhibits a pronounced peak or strong enhancement [78,79]. This behavior signals a region of reduced stiffness "softness" in the EoS, where the system becomes more easily compressible due to increased correlations and critical fluctuations near the transition temperature [81]. A detailed understanding of isothermal compressibility and its behavior during the transition is therefore essential for characterizing the EoS of strongly interacting matter and for interpreting experimental observables in RHIC [78]. When the pionic phase evolves toward the PP phase in a finite volume, such as that created at the RHIC, both the pressure and the isothermal compressibility exhibit characteristic modifications resulting from nonextensive statistical effects and finite size constraints [35,76].

In the pionic phase, pressure is generated primarily from the degrees of freedom of the hadrons and is softened by attractive interactions and resonance formation, while the isothermal compressibility remains relatively high, reflecting the ease with which a dilute hadron gas can be compressed. As the system approaches the transition region, TS characterized by the entropic parameter q-enhances high-momentum tails in the distribution functions, leading to an increase in pressure compared to the extensive ($q = 1$) case and modifying the stiffness of the EoS [76,77]. In finite systems, true thermodynamical singularities are smoothed out; consequently, instead of a divergence in the isothermal compressibility, a significant peak or increase is observed near the transition temperature, indicating increased density fluctuations and a softened EoS [78]. Upon entering the PP phase, the pressure rises more rapidly due to the liberation of quark and gluon degrees of freedom, while the isothermal compressibility decreases, indicating a stiffer medium.

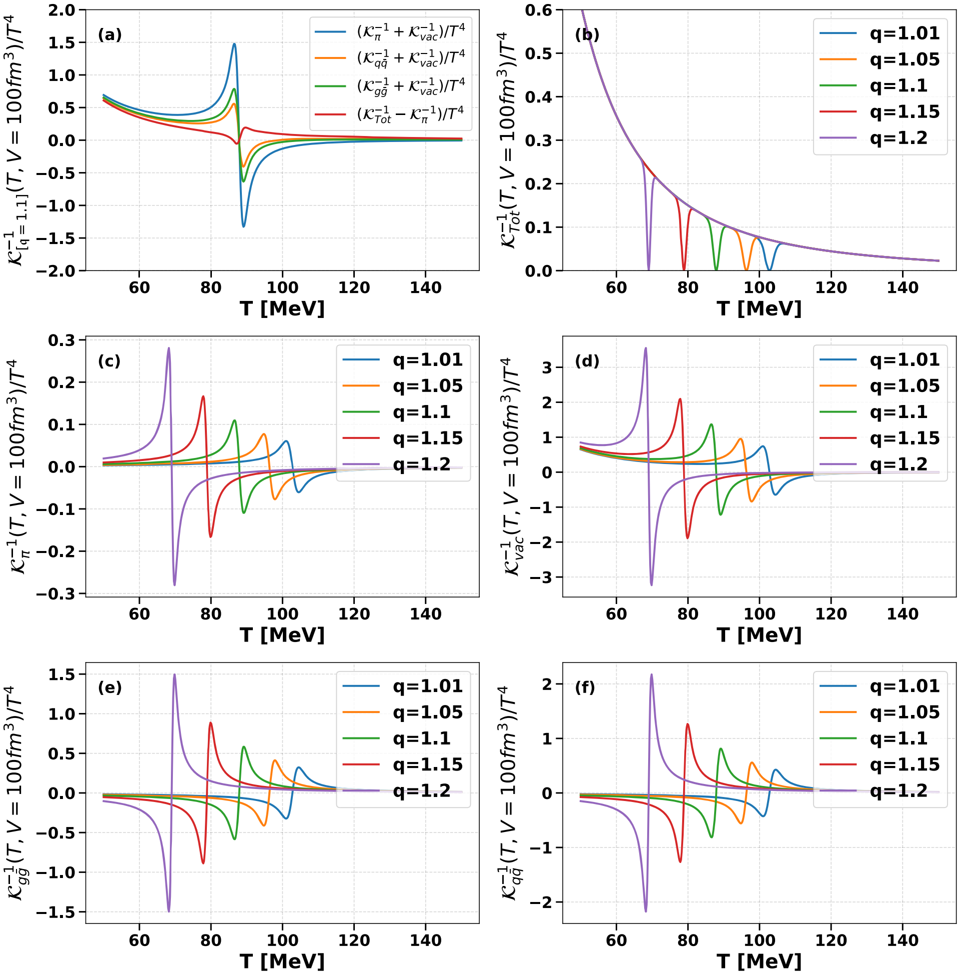

Fig. 8. (a) Vacuum compressibility, including contributions with (pion, quarks and/or gluons) compressibilities for the system, shown as a function of $(T, q = 1.1; V = (\mathrm{fm})^3)$. (b)-(f) Present the plots of the total compressibility, pions compressibility, vacuum compressibility, gluons compressibility, and quarks compressibility of the system, respectively, as functions of (q, T) at a fixed volume $V = (0.1\mathrm{fm})^3$.

Nonextensive effects tend to expand the transition region and shift the position of the compressibility peak, an effect that becomes more pronounced at finite volume, where long range correlations and incomplete equilibration are expected [35,81].

Figs. 6, 7, 8, and 9 summarize the pressure and isothermal compressibility of pions, quarks, gluons, and the QCD vacuum for a finite volume ($V = (0.1\mathrm{fm})^3$) within the nonextensive TS framework. When studying a particular subsystem (pions, vacuum, quarks, or gluons) during the operation of the entire system, the corresponding thermodynamical quantities are evaluated using the whole system expectation value defined in Eq. (19). Accordingly, Fig. 6 presents the pressure of each component calculated together with all other pressures, naturally including phase coexistence, statistical mixing, and mechanical equilibrium. In this case, the pionic contribution dominates the low-temperature region, corresponding to the negative vacuum pressure associated with the bag constant, in agreement with the MIT bag model description of confinement [29]. As the temperature increases, Tsallis nonextensive effects ($q > 1$) enhance the high momentum tails, leading to a rapid rise of quark and gluon pressures and signaling the onset of deconfinement, consistent at finite temperature QCD expectations [78]. The corresponding response of the system is shown in Fig. 8, where the isothermal compressibility is calculated along with all other components using the whole system, again via Eq. (19). In the hadronic phase, the compressibility is relatively large, indicating a soft EoS, while near the transition region a pronounced enhancement appears. At finite volumes, the true thermodynamical divergences vanish and are replaced by finite peaks, according to the finite size scaling arguments [82]. In contrast, Fig. 7 displays the pressure calculated for each individual subsystem, which corresponds to the single active component case described by Eq. (20). Thus, this figure represents all intrinsic cases of pions, vacuum, quarks, and gluons, free from collective mixing effects, and provides fundamental thermodynamical behavior. A direct comparison between Figs. 6 and 7 demonstrates thermodynamical consistency with minor differences, where the pressure of the subsystem included in the whole system coincides with its intrinsic pressure when treated independently, ensuring mechanical equilibrium between the phases [80]. Similarly, Fig. 8 shows the isothermal compressibility calculated for each subsystem with itself using Eq. (20), revealing that pions remain comparatively soft, quarks and gluons become increasingly stiff at high temperature, and the vacuum contribution is nearly temperature independent.

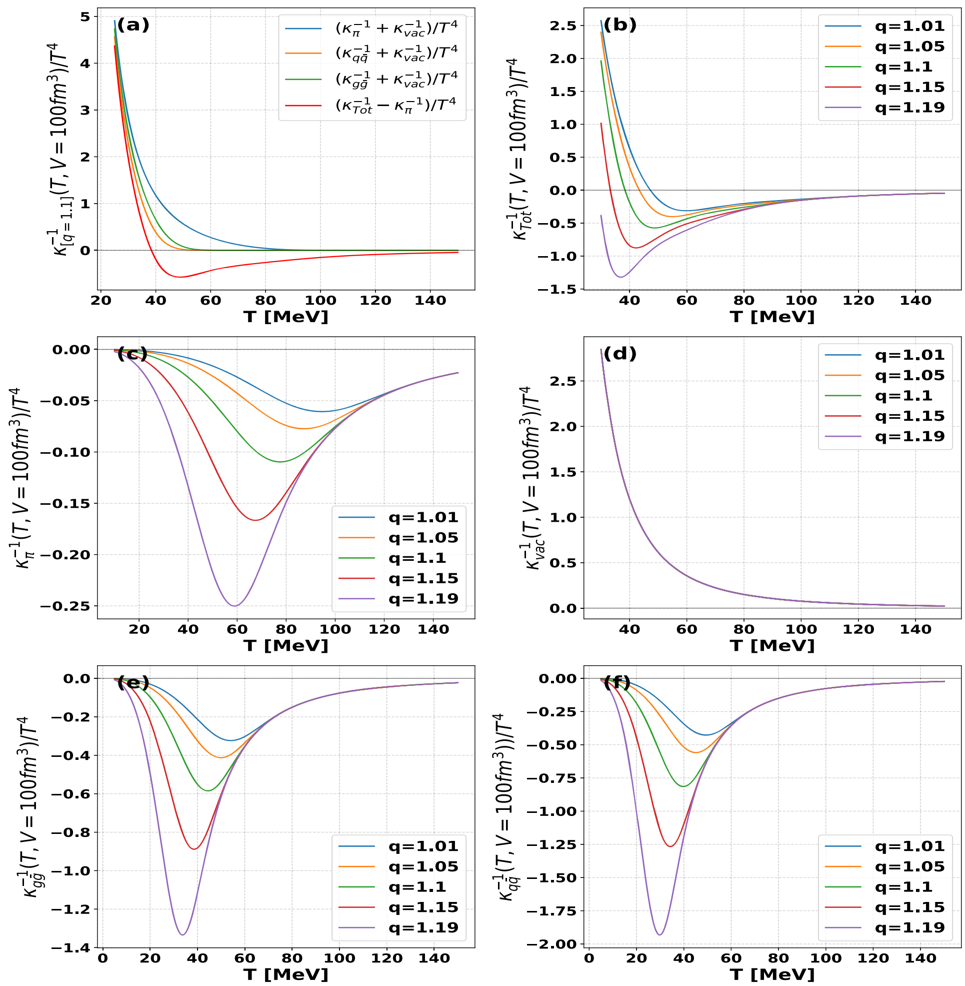

Fig. 9. (a) Vacuum compressibility, together with (pion, quark-antiquark and/or gluon-antigluon) compressibilities for the subsystem, at a fixed ($q = 1.1; V = (0.1\text{fm})^3$). (b)-(f) The plots for ($\kappa_{\text{tot}}^{-1}, \kappa_{\pi}^{-1}, \kappa_{\text{vac}}^{-1}, \kappa_{g\bar{g}}^{-1}$, and $\kappa_{q\bar{q}}^{-1}$) of the sub-system, respectively, at a fixed volume $V = (0.1\text{fm})^3$ for $q \in \{1.01, 1.05, 1.10, 1.15 \text{ and } 1.20\}$.

Because vacuum pressure is intrinsically negative due to the bag constant, the explicit negative sign in the compressibility definition, Eq. (33), is not interpreted as a physical instability; rather, it reflects the stabilizing role of the vacuum against expansion, consistent with the standard thermodynamics of the bag model [29,34]. In general, the combined behavior observed in Figs. 6, 7, 8, and 9 demonstrates that FVE smooths critical behavior, while Tsallis nonextensivity expands the transition region and enhances pressure, yielding robust thermodynamical signatures of the hadron-parton transition in small systems with strong interaction [35,76].

4. Conclusion

This work has elucidated the combined and independent roles of FVE and nonextensive TS in shaping the behavior of selected TRFs in the vicinity of the deconfinement transition from HG to PP. Our analysis shows that finite spatial confinement smooths the sharp transition characteristic of the thermodynamical limit, resulting in a gradual transition over a finite temperature range. In particular, some TRFs, such as the order parameter, energy density, pressure, and entropy density, which exhibit discontinuous or rapidly changing behavior at the transition temperature ($T_0(\infty)$) in the infinite volume limit, display a softened response when the system volume is finite.

The inclusion of nonextensive TS introduces an additional shift of the transition point at finite volume. In the absence of the colorless condition within BG, FVE at the transition point remain essentially unchanged. However, when the colorless condition is imposed, a noticeable volume-dependent shift of the transition temperature emerges, consistent with earlier studies [8,68]. By contrast, without this constraint, finite-volume corrections to the transition point become negligible.

We addressed the effect of the q-parameter on the deconfinement phase transition, as well as the various thermodynamical characteristics at finite temperatures without the chemical potential. We found that the SB limit is related to the statistics used in this work. Within TS, for example, the thermodynamical quantities $H_\mathfrak{q}$, $\varepsilon_\mathfrak{q}/T^4$, $p_\mathfrak{q}/T^4$, $s_\mathfrak{q}/T^3$, and $\theta_\mathfrak{q}/T^4$ all increase with $\mathfrak{q}$, exceed their normal SB limits, and asymptotically approach a new $\mathfrak{q}$-related Tsallis limit at sufficiently high temperatures.

The pressure and isothermal compressibility of QCD matter were analyzed in a finite volume within the nonextensive Tsallis framework, yielding a thermodynamically consistent description of the hadronic partonic transition. The resulting EoS exhibits characteristic softening and re-stiffening behavior, in agreement with theoretical expectations for strongly interacting matter at high temperature and finite chemical potential [83]. The definition of isothermal compressibility in $(2+1)$-flavor QCD is reformulated in terms of conserved charge fluctuations to enable a thermodynamically consistent characterization of mechanical stability near the crossover [22]. This framework reveals that the compressibility of strong-interaction matter along the pseudo-critical line remains remarkably close to the ideal gas limit of $1/P$ [22,84]. Consequently, this provides a unified perspective on density fluctuations and mechanical stability in finite volumes under extreme conditions. This behavior closely parallels incompressibility phenomena in finite nuclei and nuclear matter, where FVE suppress divergences while preserving clear signatures of phase transitions [84].

In this work, the FVE and Tsallis nonextensivity were treated as independent sources of deviation from the ideal thermodynamical limit. While the finite volume modifies the density of states and phase-space structure, the Tsallis parameter $\mathfrak{q}$ accounts for intrinsic fluctuations and correlations that may persist even at fixed volume. The results show that the transition point varies with the nonextensivity $\mathfrak{q}$-parameter but remains constant at a specific value of q, even for different volumes [70,77]. Furthermore, the results show that with increasing values of the Tsallis nonextensivity parameter $\mathfrak{q}$, the transition temperature decreases and the transition becomes sharper [35]. This behavior implies that stronger nonextensive effects (larger $\mathfrak{q}$) enhance deconfinement, as fluctuations and long-range correlations facilitate the formation of the QGP [85,86]. However, due to an unexpected cancellation, the $\mathfrak{q}$-parameter has no effect on the high temperature limit for $p_\mathfrak{q}/\varepsilon_\mathfrak{q}$ and $\theta_\mathfrak{q}/T^4$ [40,87].

In general, the present results are consistent with the current theoretical and experimental constraints on the EoS of dense and hot strongly interacting matter, reinforcing the relevance of compressibility and pressure as powerful tools for deconfinement [78]. In addition, TRFs have the highest response to $\mathfrak{q}$ near the transition point $T_0(V)$. Future investigations will extend this study within the TS by incorporating colorless conditions and considering the effects of the chemical potential [49].

CRediT authorship contribution statement

M.A.A. Ahmed: Writing – original draft, Software, Methodology, Investigation, Formal analysis, Conceptualization; **H. Zainuddin:** Writing – review & editing, Validation, Methodology, Investigation, Formal analysis.

Data availability

No data was used for the research described in the article.

Declaration of competing interest

The authors declare the following financial interests/personal relationships which may be considered as potential competing interests:

Mohammed Ahmed reports a relationship with Taiz University that includes: employment. If there are other authors, they declare that they have no known competing financial interests or personal relationships that could have appeared to influence the work reported in this paper.

Appendix A.

A.1. Tsallis grand canonical partition function

In the continuous case, we can write Eq. (13), so the resulting expression for the logarithm of the Tsallis grand canonical partition function of particles and antiparticles with massless and chemical potential μ and degeneracy factor g in the large volume limit of free gas is as follows:

$$\ln Z_\mathfrak{q}^{(\mathrm{BE,FD})}(V;\beta,\mu) = \frac{gV}{6\pi^2}\int_0^\infty \left[\frac{p^3}{(1+(\mathfrak{q}-1)\beta(\varepsilon\pm\mu))^{\frac{\mathfrak{q}}{\mathfrak{q}-1}}+\alpha}\right]dp. \tag{A.1}$$

Now we will go to compute the Tsallis partition function for fermion and boson:

- the Tsallis partition function of the fermi and anti-fermi gas,

$$\ln Z_\mathfrak{q}^{F\bar{F}}(V;\beta,\mu) = \frac{g_{F\bar{F}}V}{6\pi^2}\sum_{s=1}^{\infty}(-1)^{s+1}\int_0^\infty \left[\frac{p^3}{(1+(\mathfrak{q}-1)\beta(\varepsilon\pm\mu))^{\frac{s\mathfrak{q}}{\mathfrak{q}-1}}}\right]dp \tag{A.2}$$

- the Tsallis partition function of the boson and anti-boson gas,

$$\ln Z_\mathfrak{q}^{B\bar{B}}(V;\beta,\mu) = \frac{g_{B\bar{B}}V}{6\pi^2}\sum_{s=1}^{\infty}\int_0^\infty \left[\frac{p^3}{(1+(\mathfrak{q}-1)\beta(\varepsilon\pm\mu))^{\frac{s\mathfrak{q}}{\mathfrak{q}-1}}}\right]dp \tag{A.3}$$

We substitute $x = \beta(\varepsilon \pm \mu)$ in Eqs. (A.2) and (A.3):

$$I_{\mathfrak{q}}^{(\mathrm{BE,FD})}(\beta,\mu) = \begin{cases} \frac{1}{\beta}\sum_{s=1}^{\infty}(-1)^{s+1}\int_{\pm\beta\mu}^{\infty}\left[\frac{\left(\frac{x}{\beta}\pm\mu\right)^3}{(1+(\mathfrak{q}-1)x)^{\frac{s\mathfrak{q}}{\mathfrak{q}-1}}}\right]dx, & \text{for fermi case,} \\ \frac{1}{\beta}\sum_{s=1}^{\infty}\int_{\pm\beta\mu}^{\infty}\left[\frac{\left(\frac{x}{\beta}\pm\mu\right)^3}{(1+(\mathfrak{q}-1)x)^{\frac{s\mathfrak{q}}{\mathfrak{q}-1}}}\right]dx, & \text{for boson case.} \end{cases} \tag{A.4}$$

This result is produced by direct algebraic operations, as explained below:

$$I_{\mathfrak{q}}^{(\mathrm{BE,FD})}(\beta,\mu=0) = \begin{cases} \frac{\Phi\left(-1,1,\frac{4}{\mathfrak{q}}-3\right)-\Phi\left(-1,1,\frac{1}{\mathfrak{q}}\right)+3\left[\Phi\left(-1,1,\frac{2}{\mathfrak{q}}-1\right)-\Phi\left(-1,1,\frac{3}{\mathfrak{q}}-2\right)\right]}{\beta^4\mathfrak{q}(\mathfrak{q}-1)^3} = \frac{T_{\mathfrak{q}}^F}{\beta^4}, & \text{for boson,} \\ \frac{\psi^0\left(\frac{1}{\mathfrak{q}}\right)-\psi^0\left(\frac{4}{\mathfrak{q}}-3\right)+3\left[\psi^0\left(\frac{3}{\mathfrak{q}}-2\right)-\psi^0\left(\frac{1}{\mathfrak{q}}-1\right)\right]}{\beta^4\mathfrak{q}(\mathfrak{q}-1)^3} = \frac{T_{\mathfrak{q}}^B}{\beta^4}, & \text{for fermion,} \end{cases} \tag{A.5}$$

where ψ^0 is the digamma function, and Φ is the Lerch's transcendent [88]. In this work, we study the TS without chemical potential. For the HG and PP phases, the Tsallis partition function is given by,

$$\ln Z_{\mathfrak{q}}^{(\mathrm{HG,PP})}(V_{(\mathrm{HG,PP})};\beta) = \frac{g_{(\mathrm{HG,PP})}}{6\pi^2}V_{(\mathrm{HG,PP})}\beta I_{\mathfrak{q}}^{(\mathrm{HG,PP})}(\beta), \tag{A.6}$$

where $I_{\mathfrak{q}}^{(\mathrm{HG,PP})}(\beta)$ is thermal function

A.2. Gibbs grand canonical partition function of our system

Now, we will show how TS goes to BG statistics by taking $\mathfrak{q}$ tends to 1:

$$\lim_{\mathfrak{q}\longrightarrow 1} \mathcal{S}_{\mathfrak{q}}(\mathfrak{s}) = \mathcal{S}^{BG}(\mathfrak{s}), \tag{A.7}$$

and, for the partition function, we obtain

$$\lim_{\mathfrak{q}\longrightarrow 1} Z_{\mathfrak{q}}(V;\beta,\mu) = Z^{BG}(V;\beta,\mu), \tag{A.8}$$

Similarly, for the distribution of the particles i.e.

$$\lim_{\mathfrak{q}\longrightarrow 1} n_{\mathfrak{q}}(V;\beta,\mu) = n^{BG}(V;\beta,\mu). \tag{A.9}$$

The limit of $I_{\mathfrak{q}}^{(\mathrm{HG,PP})}(\beta)$ is,

$$\lim_{\mathfrak{q}\to 1} I_q^{(\mathrm{HG,PP})}(\beta) = \begin{cases} \frac{\pi^4}{15\ \beta^4}, & \text{if} \qquad \text{the particle is boson,} \\ \frac{7\pi^4}{60\ \beta^4}, & \text{when} \qquad \text{the particle is fermion.} \end{cases} \tag{A.10}$$

The result in Eq. (16) was obtained when we separated the parts biased by the volume fraction parameter h together, and we repeated this process for the other parts. This result will be the same as that gotten in the BG when $\mathfrak{q} \longrightarrow 1$, so the limit of Eq. (16) at this value reads,

$$\lim_{\mathfrak{q}\to 1} \ln Z_{\mathfrak{q}}^{\mathrm{SYS}}(h,V;T) = VT^3\left[\left(\frac{37}{90}\pi^2 - \frac{\mathfrak{B}}{T^4}\right) + \left(\frac{\mathfrak{B}}{T^4} - \frac{17}{45}\pi^2\right)h\right]. \tag{A.11}$$

References

[1] A. Andronic, et al., Heavy-flavour and quarkonium production in the LHC era: from p-p to heavy-ion collisions, Eur. Phys. J. C 76 (2016) 0107.
[2] S. Sarkar, S. Helmut, S. Bikash, The Physics of the QGP, Introductory Lectures, Springer Verlag, (2009).
[3] E. Shuryak, Strongly coupled QGP in heavy ion collisions, Rev. Mod. Phys. 89 (2017) 035001.
[4] J. Cleymans, R. Gavai, E. Suhonen, Quarks and gluons at high temperatures and densities, Phys. Rep. 130 (1996) 217–292.
[5] S. Ejiri, et al., Isentropic equation of state of 2-flavor QCD, Phys. Rev. D 73 (2006) 054506.
[6] M. Cheng, et al., QCD equation of state with almost physical quark masses, Phys. Rev. D 77 (2008) 014511.
[7] R. Claudia, P. Lattice, QCD and heavy ion collisions: a review of recent progress, Rep. Prog. Phys. 81 (2018) 084301.
[8] A. Shaikh, K. Ranjita, S. Datta, QCD phase diagram and the finite volume fireball: a model study, Nucl. Phys. A 1054 (2025) 375–9474.
[9] I. Etsuko, Lattice Results for the Equation of State in Dense QCD-like Theories, Universe 11, (2025) 380.
[10] K. Michael, Monte Carlo methods in statistical physics: mathematical foundations and strategies Commun. Nonlinear Sci. 15 (2010) 1589–1602.
[11] J. Gasser, H. Leutwyler, Thermodynamics of chiral symmetry, Phys. Lett. B 188 (1987) 477–481.
[12] K. Binder, Applications of monte carlo methods to statistical physics, Rep. Prog. Phys. 60 (1997) 487.
[13] P. Somenath, et al., Effect of finite volume on thermodynamics of quark-hadron matter, Phys. Rev. D 109 (2024) 014009.
[14] J. Kapusta, Finite-Temperature Field Theory Principles and Applications, Cambridge Publishing Company, (2006).
[15] C. Spieles, H. Stöcker, C. Greiner, Phase transition of a finite QGP, Phys. Rev. C 57 (1998) 908–915.
[16] A. Anton, et al., Decoding the phase structure of QCD via particle production at high energy, Nature 561 (2018) 321–330.

[17] B. Szabolcs, W. Collaboration, Thermodynamics of the QCD transition from lattice, Nucl. Phys. A 904 (2013) 270c–277c.
[18] A. Dragoa, A. Lavagno, P. Quarati, Nonextensive statistical effects on the relativistic nuclear equation of state, Physica A 344 (2004) 472–477.
[19] A. Teweldeberhan, H. Miller, R. Tegen, Generalized statistics and the formation of a QGP, Int. J. Mod. Phys. E 12 (2003) 395.
[20] F. Pereira, R. Silva, J. Alcaniz, Nonextensive effects on the relativistic nuclear equation of state, Phys. Rev. C 76 (2007) 015201.
[21] A. Lavagno, D. Pigato, P. Quarati, Nonextensive statistical effects in the hadron to QGP transition, J. Phys. G 37 (2010) 115102.
[22] D. Clarke, et al., A Generalized Definition of the Isothermal Compressibility in (2 + 1)-Flavor QCD, Phys. Rev. D 113 (2026) 034502.
[23] G. Sourendu, N. Karthik, P. Majumdar, On criticality and the equation of state of QCD at finite chemical potential, Phys. Rev. D 90 (2014) 034001.
[24] M. Eugenio, et al., Tsallis statistics and thermofractals: applications to high energy and hadron physics, Int. J. Mod. Phys. A 38 (2023) 2341004.
[25] R. Gupta, A. Menon, S. Jain, S. Jena, The Theoretical Description of the Transverse Momentum Spectra: A Unified Model, Universe 9 (2023) 111.
[26] M. Rybczyński, Z. Wlodarczyk, Tsallis statistics approach to the transverse momentum distributions in p-p collisions, Eur. Phys. J. C 74 (2014) 2785.
[27] T. Bhattacharyya, A. Mukherjee, Propagation of nonlinear waves in hot, ideal, and non-extensive QGP, Eur. Phys. J. C 80 (2020) 656.
[28] O. Juliana, et al., Non-extensive statistics in au-Au collisions, Phys. Lett. B 854 (2024) 138727.
[29] A. Chodos, et al., New extended model of hadrons, Phys. Rev. D 9 (1974) 3471.
[30] T. Degrand, J. Robert, K. Johnson, J. Kiskis, Masses and other parameters of the light hadrons, Phys. Rev. D 12 (1975) 2060.
[31] F. Karsch, Thermodynamic properties of strongly interacting matter at non-zero baryon number density, J. Phys. G 31 (2005) 633–S640.
[32] F. Vanesa, et al., Masses of hadrons, tetraquarks, and pentaquarks through a Tsallis entropy approach in the MIT bag model, Entropy 27 (2025) 681.
[33] S. Hasmik, T. Sargsyan, A. Babajanyan, Maximal mass strange quark stars based on the modified MIT model with variable vacuum pressure, Nucl. Phys. B 1022 (2026) 117277.
[34] J. Salil, S. Sau, S. Sanyal, Quark cores in extensions of the MIT bag model, JHEA 30 (2021) 16–23.
[35] C. Tsallis, Possible generalization of Boltzmann-Gibbs statistics, J. Stat. Phys. 52 (1988) 479–487.
[36] G. Wilk, Z. Włodarczyk, Interpretation of the nonextensivity parameter q in some applications of Tsallis statistics and lévy distributions, Phys. Rev. Lett. 84 (2000) 2770–2773.
[37] C. Beck, Non-extensive statistical mechanics and particle spectra in elementary interactions, Physica A 286 (2000) 164–180.
[38] A. Deppman, Self-consistency in non-extensive thermodynamics of highly excited hadronic states, Physica A 391 (2012) 6380–6385.
[39] L. Marques, J. Cleymans, A. Deppman, Description of high energy p-p collisions using Tsallis thermodynamics: transverse momentum and rapidity distributions, Phys Rev D 91 (2015) 054025.
[40] Y.P. Zhao, Thermodynamic properties and transport coefficients of QCD matter within the nonextensive PNJL model, Phys. Rev. D 101 (2020) 096006.
[41] A. Lavagno, Relativistic nonextensive thermodynamics, Phys. Lett. A 301 (2002) 13–18.
[42] H. Satz, Probing the states of matter in QCD, Int. J. Mod. Phys. A 28 (2013) 1330043.
[43] K. Kyan, A. Monnai, QCD equation of state with tsallis statistics for heavy-ion collisions, Phys. Rev. D 106 (2022) 054004.
[44] Q. Zhi-Ying, et al., QCD phase transition at finite temperature and chemical potential with nonextensive statistics, Phys. Rev. D 112 (2025) 096022.
[45] C. Tsallis, Nonadditive entropy: the concept and its use, Eur. Phys. J. A 40 (2009) 257–266.
[46] A. Lavagno, Basic-deformed quantum mechanics, Rept. Math. Phys. 64 (2009) 79–91.
[47] F. Brito, A. Marinho, Q-Deformed landau diamagnetism problem embedded in D-dimensions, Phys A 390 (2011) 2497–2503.
[48] W. Johnson, Some applications of the q-exponential formula, Dis Math. 157 (1996) 207–225.
[49] J. Zhang, J. Wen, Stability analysis of magnetized quark matter in Tsallis statistics, Universe 11 (2025) 312.
[50] D. Singh, A. Kumar, Thermodynamic properties and phase diagram of quark matter within non-extensive polyakov chiral SU(3) quark mean field model, Chinese Phys. C 48 (2024) 053103.
[51] N. Nelson, Open problems within nonextensive statistical mechanics Entropy 26 (2024) 118.
[52] J. Willard, Gibbs Elementary Principles in Statistical Mechanics: The Rational Foundation of Thermodynamics, Cambridge, University Press John Wilson and Son, (2010).
[53] D. Ruelle, Statistical Mechanics: Rigorous Results, Springer, (1999).
[54] K. Arvind, et al., Speed of sound in hadronic matter using non-extensive Tsallis statistics, Eur Phys J. A 52 (2016) 292.
[55] W. Alberico, A. Lavagno, P. Quarati, Non-extensive statistics, fluctuations and correlations in high-energy nuclear collisions, Eur. Phys. J. C 12 (2000) 499–506.
[56] C. Tsallis, R. Mendes, A. Plastino, The role of constraints within generalized nonextensive statistics, Physica A 261 (1998) 534–554.
[57] H. Hasegawa, Bose-Einstein and fermi-Dirac distributions in nonextensive quantum statistics: exact and interpolation approaches, Phys. Rev. E 80 (2009) 011126.
[58] S. Mitra, Thermodynamics and relativistic kinetic theory for q-generalized bose-Einstein and fermi-Dirac systems, Eur. Phys. J. C 78 (2018) 66.
[59] J. Conroy, H. Miller, A. Plastino, Thermodynamic consistency of the q-deformed fermi-Dirac distribution in nonextensive thermostatics, Phys. Lett. A 374 (2010) 4581–4584.
[60] J. Conroy, H. Miller, Color superconductivity and Tsallis statistics, Phys. Rev. D 78 (2008) 054010.
[61] A. Teweldeberhan, A. Plastino, H. Miller, On the cut-off prescriptions associated with power-law generalized thermostatistics, Phys. Lett. A 343 (2004) 71–78.
[62] F. Pennini, A. Plastino, A.R. Plastino, Tsallis entropy and quantal distribution functions, Phys. Lett. A 208 (1995) 309–314.
[63] A. Shalaby, V. Oikonomou, G. Nashed, Non-Extensive Thermodynamics Effects in the Cosmology of f(T) Gravity, Symmetry 13 (2021) 1–16.
[64] F. Büyükkiliç, D. Demirhan, A fractal approach to entropy and distribution functions, Phys. Lett. A 181 (1993) 24–28.
[65] J. Torres, D. Menezes, Quark matter equation of state and stellar properties, Europhys. Lett. 101 (2013) 42003.
[66] M. Fisher, M. Barber, Scaling theory for finite-size effects in the critical region, Phys. Rev. Lett. 28 (1972) 1516–1519.
[67] K. Binder, Finite size scaling analysis of ising model block distribution functions, Zeitschrift für 1981, Phys. B. 43 (1981) 119–140.
[68] M. A. A. Ahmed, et al., Finite-volume cumulant expansion in QCD-colorless plasma, Eur. Phys. J. C 75 (2015) 431.
[69] M. A. A. Ahmed, et al., Detailed study of the QCD equation of state of a colorless partonic plasma in finite volume, Int.J. Mod. Phys. A 34 (2019) 1950051.
[70] S. Salah, et al., Finite-size effects and finite-size scaling in time evolution during a colorless confining phase transition, Phys. Scr. 96 (2021) 105302.
[71] R. Feynman, Statistical Mechanics: A Set of Lectures, The Benjamin Cummings Publishing Comapny, (1982).
[72] R. Balian, From Microphysics to Macrophysics: Methods and Applications of Statistical Physics Edition, Springer Verlag, (2007).
[73] B. Carolina, G. Corral, Quark matter description in a Tsallis entropy approach, Eur Phys. J. A 55 (2019) 146.
[74] R. Jacek, G. Wilk, Nonextensive quasiparticle description of QCD matter, Symmetry 11 (2019) 401.
[75] C. Barter, D. Blaschke, H. Voss, Thermodynamics of quark matter with saturated confinement interactions, Phys. Lett. B 293 (1992) 423–429.
[76] J. Cleymans, D. Worku, Relativistic thermodynamics: transverse momentum distributions in high-energy physics, Eur. Phys. J. A 48 (2012) 160.
[77] J. Rożynek, G. Wilk, Nonextensive effects in the NJL model of QCD, J. Phys. G 36 (2009) 125108.
[78] P. Braun-Munzinger, J. Wambach, Colloquium: phase diagram of strongly interacting matter, Rev. Mod. Phys. 81 (2009) 1031–1050.
[79] A. Bazavov, et al., Equation of state in (2 1)-flavor QCD, Phys. Rev. D 90 (2014) 094503.
[80] B. Callen, Thermodynamics and an Introduction to Thermostatistics, Wiley, (1985).
[81] M. Stephanov, QCD phase diagram and the critical point, Prog. Theor. Phys. Suppl. 153 (2004) 139.
[82] K. Binder, D. Landau, Finite-size scaling at first-order phase transitions, Phys. Rev. B 30 (1984) 1477–1485.
[83] C.W. Ma, Y.G. Ma, Shannon information entropy in heavy-ion collisions, Prog. Part. Nucl. Phys. 99 (2018) 120–158.
[84] J. Blaizot, Nuclear compressibilities, Phys. Rep. 64 (1980) 171–248.
[85] T. Bhattacharyya, J. Cleymans, S. Mogliacci, Nonextensive nuclear liquid gas phase transition, Phys. Rev. D 94 (2016) 094026.
[86] A. Lavagno, D. Pigato, Nonextensive nuclear liquid-gas phase transition, Physica A 392 (2013) 5164–5171.
[87] S. Dhananjay, A. Kumar, Finite size effects on the transport coefficients of strongly interacting QCD matter, Phys. Rev. D 111 (2025) 074017.
[88] A. Erdélyi, W. Magnus, F. Oberhettinger, F. Tricomi, Higher Transcendental Functions, Vol. 1, New York, Krieger, (1981), Read more in 1.7 for the digamma function and in 1.11 for Lerch's transcendent.